2021 43rd Annual International Conference of the
IEEE Engineering in Medicine & Biology Society (EMBC)
Oct 31 - Nov 4, 2021. Virtual Conference

Evaluation of Amorphous Silicon Carbide on Utah Electrode Arrays by Thermal Accelerated Aging*

Christopher K. Nguyen, *Student Member*, *IEEE*, Justin R. Abbott, Sandeep Negi, and Stuart F. Cogan, *Member*, *IEEE*

***Abstract*— Long-term microelectrode arrays (MEAs) are essential devices for studying neural activity and stimulating neurons for treating neurological disorders or for recording neural activity to control prosthesis. However, practical use of MEAs is impeded by unreliable chronic stability inside the host body. We are proposing to implement amorphous silicon carbide (a-SiC) as a replacement for the current standard practice of using Parylene-C encapsulation on commercial Utah electrode arrays (UEAs) manufactured by Blackrock Neurotech. By using thermal accelerated aging (TAA), we can theoretically evaluate the lifetime stabilities in comparatively short time. After 255 days at 87°C in phosphate-buffered saline (PBS), a device has theoretically reached ~22 years at 37°C in PBS. We report on a study of an a-SiC UEA using stability criteria of impedance (Z_{1kHz} < 70 kΩ) and cathodal charge storage capacity (CSC_c > 10 mC/cm^2). At 255 days, no total electrode failures have been observed.**

***Clinical Relevance*— This research demonstrates the suitability of a-SiC to encapsulate MEAs during under long-term stability in saline environments.**

I. Introduction

Chronically implantable microelectrode arrays (MEAs) for recording and stimulation have grown in demand for neural research and emerging clinical applications. MEAs have been used as intracortical implants for brain-computer-interfaces, neuromodulation treatments, volitional control with sensory feedback of prosthetic limbs, and operating assistive devices for communication. Despite these capabilities and ongoing research, penetrating MEAs have yet to maintain satisfactory reliability necessary for long-term applications for the lifetime of patients.

MEAs are challenged by inconsistent chronic neural recording due to waning quantity and quality of neural signals [1]. One major source for progressive failing performance is the degradation of encapsulation. In this study, we use Utah electrode arrays (UEAs)—a 3D silicon-based devices and the first FDA-approved intracortical implant for investigational device exemption studies. While smaller feature sized MEAs are under development, they have not yet been used clinically. However, like all MEAs, UEAs have yet to demonstrate long-term stable implantation that matches patient lifetime. While Parylene-C is a common medical device coating, recent studies have shown that Parylene-C is vulnerable to electrolyte penetration, microcracks, and delamination [2]–[4]. In this study, we examined the use of amorphous silicon carbide (a-SiC) as an alternative electrical encapsulation for UEAs through a thermal accelerated aging (TAA) study.

II. Methods

UEAs are commercially manufactured by Blackrock Neurotech with Parylene-C as their standard practice for encapsulation. These MEAs have emerged as the leading standard for neural interface research and a core technology for clinical studies.

A. Device Fabrication

The fabrication process of 10×10 configured UEAs (4×4 mm^2) by Blackrock Neurotech is described by Bhandari *et al*., see Fig. 1(a) [5]. a-SiC film, shown in Fig. 1(b), was deposited via plasma-enhanced chemical vapor deposition (PECVD) on a Plasma-Therm Unaxis 790 Series PECVD system using deposition parameters of 325°C, 1000 mTorr, and 200 W, 1:3 gas ratio of SiH_4:CH_4, and 800 sccm Ar [6]. The UEAs are punctured through a Parylene-C-coated, thin sheet of Al foil as a hard mask so that only exposed tips undergo reactive ion etching (RIE). We removed a-SiC from the exposed tips to reveal electrode sites of UEAs in a RIE system, using etch parameters of 200 mTorr, 200 W, and 26 sccm SF_6. The foil covered UEAs are then coated with sputtered iridium oxide film (SIROF) in an AJA ATC 2200 DC magnetron sputtering system to deposit electro-active coatings at the electrode site, depicted in Fig. 1(b). A 60-nm Ti adhesion layer was sputtered at 4 mTorr, 200 W, and 50 sccm Ar; a 250-nm SIROF layer was sputtered at 30 mTorr, 100 W, 1:3 gas ratio of O_2: H_2O, and 20 sccm Ar [7]. Individual UEAs were diced into 4×4 configuration, shown in Fig. 1 (c). In Fig. 1(e)-(f), 4×4 configured UEAs (2×2 mm^2) were bonded to Au wire bundles that were connected to printed circuit boards (PCBs) and encapsulated in biocompatible epoxy.

A. Thermal Accelerated Aging Setup

TAA involves exposing a sample to higher temperature than normally used in order to induce accelerate aging—assuming Arrhenius behavior under the presumption that the sample undergoes a first-order degradation process. TAA is a commonly used reliability test to evaluate the shelf-life of drugs and the stability of medical devices [8]. This aging method has been used previously by Lei *et al*. for soak tests of a-SiC, SiO_2, and Si_3N_4 in phosphate-buffered saline (PBS) at

*Research supported by NIH SBIR Grant Number: 4R44DC018261-02.

S. Negi is with Blackrock Microsystem, Salt Lake City, UT 84108 USA. He is also with the Electrical and Computer Engineering Department, University of Utah, Salt Lake City, UT 84112 USA.

C. K. Nguyen, J. R. Abbott, and S. F. Cogan are with the Bioengineering Department, University of Texas at Dallas, Richardson, TX 75080 USA. Corresponding author: C. K. Nguyen (phone: 469-226-1740; e-mail: christopher.nguyen7@utdallas.edu).

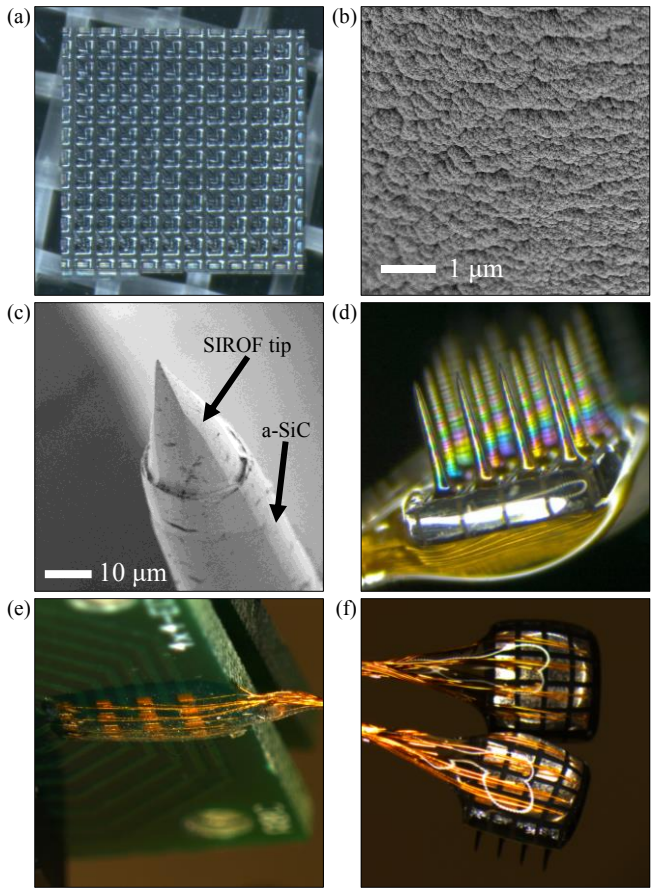

Figure 1. 4×4 configuration of UEA for small animal application, made from separated 10×10 UEA. Optical image of the received (a) 100-shank UEA. Scanning electron micrographs (SEMs) of (b) a-SiC film from the shaft tip at an angle and (c) SIROF and a-SiC. Optical images of (d) 16-shank UEA, and Au wire bonding in epoxy to (e) a PCB connected to (f) metallized backside of UEA.

87°C up to 120 days [9]. The rate constant k for the degradation reaction is given by:

$$k = A \exp\left(-\frac{E_a}{RT}\right) \quad (1)$$

Equation (1) is the Arrhenius equation, where A is the pre-exponential factor, E_a is the activation energy, R is the gas constant, and T is the absolute temperature. The ratio of rate constants is readily obtained as:

$$\frac{k_{acc}}{k_{ref}} = \exp\left(\frac{E_a}{R}\left(\frac{1}{T_{ref}} - \frac{1}{T_{accel}}\right)\right) \quad (2)$$

Equation (2) is the integrated form of the Arrhenius equation, where T_{ref} and T_{acc} are the absolute reference and acceleration temperatures, respectively, and k_{ref} and k_{acc} are the respective rate constants. TAA utilizes the "10-degree" rule, where every increment ($\theta = 10$ K) results in magnifying the reaction rate by a factor of 2:

$$\theta = 10\text{ K} \rightarrow \frac{k_{acc}}{k_{ref}} = 2 \quad (3)$$

$$A_f = 2^{\Delta T/\theta} \quad (4)$$

Equation (4) is the acceleration factor based on the temperature difference (ΔT) and the assumed difference in rate constants between these temperatures. With the human physiological temperature (37°C) as reference and utilizing acceleration temperature of 87°C, the temperature-dependent acceleration factor ($A_f = 32$) indicates that 24 hours at 87°C is 32 days at 37°C [10]. The devices are soaked in PBS (pH 7.2) for aging studies.

B. Electrochemical Characterization

To evaluate the long-term stability of a-SiC-encapsulated UEAs, electrochemical measurements were performed periodically to monitor a-SiC encapsulation integrity. All electrochemistry was performed with a Gamry Potentiostat 1000E in a three-electrode configuration in air-equilibrated PBS—using Ag|AgCl as the reference electrode and a large area Pt wire as the counter electrode. Electrochemical impedance spectroscopy (EIS) was utilized to measure electrode impedance from 10^{-1} to 10^5 Hz. Cyclic voltammetry (CV) measurements were created by potential cycling within the water electrolysis window of SIROF (-0.6 to 0.8 V). All CV measurements were taken at a sweep rate of 50 mV/s—a slow enough scan rate to access the entirety of the SIROF coating on the electrode tip and to allow for identification of oxidation-reduction waves associated with SIROF [11]. CVs were used to determine the charge stored in the electrodes during potential cycling, given by the following equation:

$$\text{CSC}_c = \frac{1}{A_{gs}} \int_0^{t_{cycle}} i_c(t)\, dt \quad (5)$$

The cathodal charge storage capacity (CSC_c) was calculated from the integral of cathodal current (i_c) as a function time (t) over one complete potential cycle (t_{cycle}) as a ratio to the geometric surface area (A_{gs}) of the electrode, namely the SIROF coating.

C. Statistical Analysis

All figure plots and regression analyses were generated in GraphPad Prism 8. This study used a single a-SiC-encapsulated UEA with $n = 16$ electrodes (technical replicates) to undergo TAA.

III. Results

This experiment reached 255 days in PBS at 87°C, which corresponds with ~22 years in PBS at 37°C. We observed variations in the stability of our sample.

A. Electrochemical Impedance Spectroscopy

Representative EIS data for one electrode (Fig. 2(a)) shows an increase in low frequency impedance (<10^{-1} Hz), indicating that there may not be Si exposure, and is consistent with an absence of increasing electrolyte leakage pathways. At high frequency (10^5 Hz) in Fig. 2(a), the impedance is unchanged with soak time, suggesting no change in the exposed geometric surface area of the electrode—no apparent damages to the SIROF. Table 1 shows the average progress at certain points of time of one UEA, where the Z_{1kHz} increases from 1.97 ± 0.38 kΩ at Day 0 to 7.47 ± 1.05 kΩ at Day 255 (linear regression analysis: $y = 0.02x + 2.44$, $R^2 = 0.32$). At low frequency, reduction in impedance indicates exposure of the underlying Si substrate while at high frequency, increase in impedance indicates damage or delamination to the electrode [12]. Table 1 however, shows that Z_{100mHz} increased from 0.48

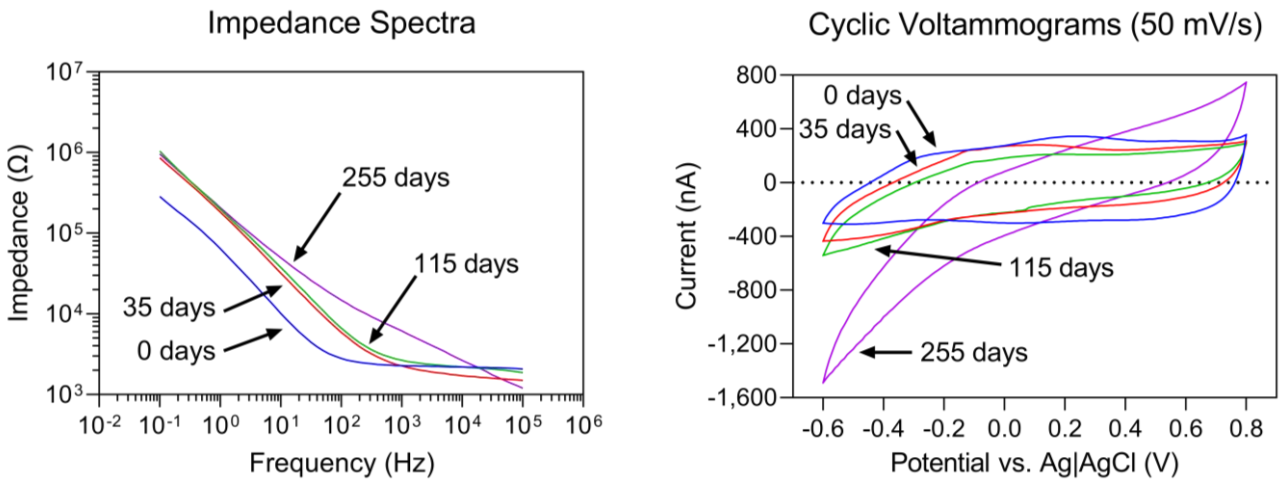

(a) (b)

Figure 2. Single representative on one electrode of a UEA. (a) Impedance spectra from 10^{-1} to 10^{5} Hz. (b) Voltammograms with 50 mV/s sweep rate. Legend is actual days soaked in PBS at 87°C: **blue** for 0 days, **red** for 35 days, **green** for 115 days, and **purple** for 255 days. The approximate respective theoretical time in PBS at 37°C is 0 years, 3 years, 10 years, and 22 years.

± 0.11 MΩ at Day 0 to 2.36 ± 1.07 MΩ at Day 255 (linear regression analysis: $y = 0.009x + 0.87$, $R^2 = 0.40$). Table 1 also shows that $Z_{100\text{kHz}}$ reduced from 1.69 ± 0.34 kΩ at Day 0 to 1.13 ± 0.37 kΩ at Day 255 (linear regression analysis: $y = -0.35x + 2.20$, $R^2 = 0.16$). Fig. 4 illustrates the present stability of the UEA at the three frequencies of interest.

B. Cyclic Voltammetry

Fig. 2(b) depicts the CV current response at 50 mV/s sweep rate as a function of aging time on a representative electrode. The CV current response progressively increases as the UEA undergoes aging. The CV is also the immediate step into the investigation of CSC_c. From Table 1, CSC_c increased from 40.25 ± 5.15 mC/cm^2 at Day 0 to 56.04 ± 21.00 mC/cm^2 at Day 255 (linear regression analysis: $y = 0.06x + 31.85$, $R^2 = 0.14$). Fig. 4 illustrates the changes of CSC_c over time.

IV. Discussion

Although other dielectric materials are used in MEA insulation, a-SiC provides superior long-term electrical encapsulation. Two commonly used dielectric materials in semiconductor industry and MEA fabrication are silicon dioxide (SiO_2) and silicon nitride (Si_3N_4). While SiO_2 and Si_3N_4 are good dielectrics in electronics, Lei *et al*. observed noticeable dissolution when submerged in electrolyte over time unlike a-SiC [9]. This UEA that underwent TAA exhibited the capability of a-SiC as a stable dielectric material. $Z_{1\text{kHz}}$ remained under our 70 kΩ threshold, suitable impedance for neural recording and stimulation with SIROF electrodes [7], [13], [14], and CSC_c maintained our goal of at least 10 mC/cm^2. The impedance at 1 kHz is typically defined as the characteristic frequency of action potentials [15]. The drastic increase in $Z_{1\text{kHz}}$ starting at Day 213 in Fig. 3 could be caused by oxidation of the Si substrate underneath the SIROF. We do not believe that this increase is due to the delamination of SIROF as the CSC_c in Fig. 4 describes the SIROF coating to be relatively stable. Also, the non-increasing $Z_{100\text{kHz}}$ indicates that there is no noticeable delamination of SIROF. The noticeable reduction in $Z_{100\text{mHz}}$ starting at Day 241 may be associated with Si substrate exposure; however, this Si substrate expsoure may not have originated from the a-SiC encapsulated side. Day 255 in Fig. 2(b) indicates low frequency leakage pathway development such that the tilt in the CV can represent a possible resistive pathway formation. A possible cause for onset of leakage is the dissolution of the epoxy, resulting in leakage from the backside of UEAs. We will need to perform scanning electron microscopy (SEM) to examine any physical failure modes.

While TAA is a useful *in vitro* test method that gauges stability, TAA does not provide sufficient conditions to simulate a biological environment. Therefore, we may consider implementing an additional mode of aging such as adding H_2O_2 to simulate reactive oxygen species from cortical immune response. Takmakov *et al*. developed an automated TAA system that maintained a constant concentration of H_2O_2—called reactive accelerated aging (RAA)—and they tested on Parylene-C-encapsulated UEAs [16]. However, there is no established A_f in RAA as there was rapid degradation of Parylene-C in Caldwell *et al*., preventing development of a quantifiable aging scale [17]. To better simulate electrically

TABLE I. Representative aging data for an a-SiC-encapsulated UEA ($\bar{x} \pm s$, $n = 16$ electrodes).

Time		Impedance			Charge Storage Capacity (mC/cm^2)
Actual at 87°C (days)	*Theoretical at 37°C (years)*	*At 100 mHz (MΩ)*	*At 1 kHz (kΩ)*	*At 100 kHz (kΩ)*	
0	0	0.48 ± 0.11	1.97 ± 0.38	1.69 ± 0.34	40.25 ± 5.15
35	3	1.08 ± 0.27	3.52 ± 2.22	1.95 ± 0.67	34.01 ± 7.15
115	10	2.27 ± 0.84	3.95 ± 1.72	2.11 ± 0.56	42.34 ± 8.41
255	22	2.36 ± 1.07	7.47 ± 1.05	1.13 ± 0.37	56.04 ± 21.00

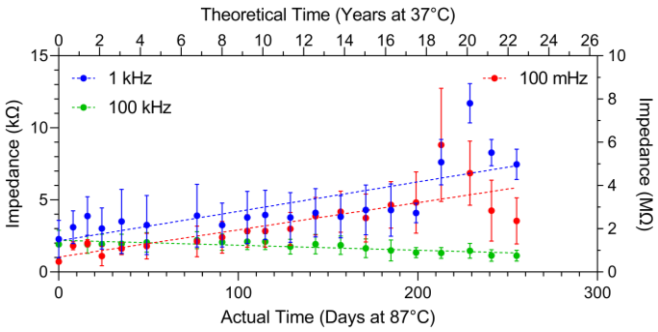

Figure 3. Representative Z_{100mHz}, Z_{1kHz}, and Z_{100kHz} of one UEA ($\bar{x} \pm s$, $n = 16$ electrodes). Impedance at 100 mHz (MΩ) is **red**, 1 kHz (kΩ) is **blue**, and 100 kHz (kΩ) is **green**. The lower x-axis is the actual time soaked in PBS at 87°C while the upper x-axis is the accelerated time soaked in PBS at 37°C. Dashed lines are trendlines generated by linear regression analysis.

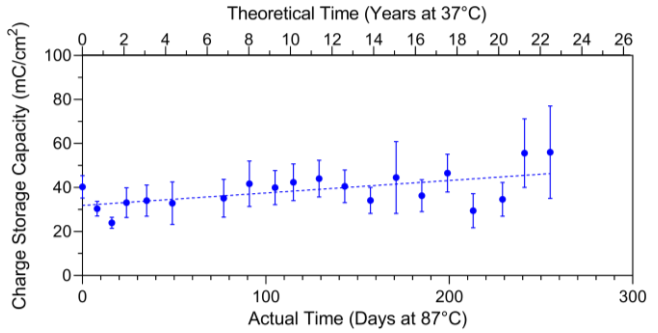

Figure 4. Representative CSC_c of one UEA ($\bar{x} \pm s$, $n = 16$ electrodes). The lower x-axis is the actual time soaked in PBS at 87°C while the upper x-axis is the accelerated time soaked in PBS at 37°C. Dashed lines are trendlines generated by linear regression analysis.

driven degradation, electrical accelerated aging (EAA) should be considered, which uses voltage as a mode of stress to cause accelerated aging. EAA a common reliability test that to evaluate dielectric properties of materials and the lifetime of electronic devices [18], [19]. Future studies of a-SiC encapsulation will employ EAA to determine susceptibility to voltage-driven breakdown in comparison to other common insulation materials.

V. Conclusion

We performed an accelerated aging study on a-SiC-encapsulated UEAs—255 days at 87°C (~22 years at 37°C). This TAA experiment demonstrated that a-SiC-encapsulated UEAs may be capable of chronic stability in saline electrolytes. Changes in electrochemical measurements may not actually express a-SiC encapsulation failures such that: (1) decreasing low frequency impedance may be caused by leakage pathway developing from the backside via epoxy dissolution and (2) increasing impedance at 1 kHz could be oxidation of the Si substrate since slow sweep rate CSC_c is relatively stable.

Disclaimer

S. Negi has a financial interest in the company Blackrock Microsystems, which develops and produces implantable neural interfaces that were used in this study.

References

[1] J. C. Barrese *et al.*, "Failure mode analysis of silicon-based intracortical microelectrode arrays in non-human primates," *J. Neural Eng.*, vol. 10, no. 6, 2013.

[2] J. M. Hsu, L. Rieth, S. Kammer, M. Orthner, and F. Solzbacher, "Effect of Thermal and Deposition Processes on Surface Morphology, Crystallinity, and Adhesion of Parylene-C," *Sensors Mater.*, vol. 20, no. 2, p. 87, 2008.

[3] W. Li, D. C. Rodger, E. Meng, J. D. Weiland, M. S. Humayun, and Y.-C. Tai, "Wafer-Level Parylene Packaging With Integrated RF Electronics for Wireless Retinal Prostheses," *J. Microelectromechanical Syst.*, vol. 19, no. 4, pp. 735–742, 2010.

[4] S. Minnikanti *et al.*, "Lifetime assessment of atomic-layer-deposited Al2O3–Parylene C bilayer coating for neural interfaces using accelerated age testing and electrochemical characterization," *Acta Biomater.*, vol. 10, no. 2, pp. 960–967, 2014.

[5] R. Bhandari, S. Negi, and F. Solzbacher, "Wafer-scale fabrication of penetrating neural microelectrode arrays," *Biomed. Microdevices*, vol. 12, no. 5, pp. 797–807, 2010.

[6] A. Joshi-Imre *et al.*, "Chronic recording and electrochemical performance of amorphous silicon carbide-coated Utah electrode arrays implanted in rat motor cortex," *J. Neural Eng.*, vol. 16, no. 4, p. 046006, 2019.

[7] J. Maeng *et al.*, "High-charge-capacity sputtered iridium oxide neural stimulation electrodes deposited using water vapor as a reactive plasma constituent," *J. Biomed. Mater. Res. Part B Appl. Biomater.*, vol. 108, no. 3, pp. 880–891, 2020.

[8] K. J. Hemmerich, "General aging theory and simplified protocol for accelerated aging of medical devices," *Med. Plast. Biomater.*, vol. 5, pp. 16–23, 1998, [Online]. Available: https://www.mddionline.com/design-engineering/general-aging-theory-and-simplified-protocol-accelerated-aging-medical-devices.

[9] X. Lei *et al.*, "SiC protective coating for photovoltaic retinal prosthesis," *J. Neural Eng.*, vol. 13, no. 4, 2016.

[10] D. W. L. Hukins, A. Mahomed, and S. N. Kukureka, "Accelerated aging for testing polymeric biomaterials and medical devices," *Med. Eng. Phys.*, vol. 30, no. 10, pp. 1270–1274, 2008.

[11] S. F. Cogan, "Neural Stimulation and Recording Electrodes," *Annu. Rev. Biomed. Eng.*, vol. 10, no. 1, pp. 275–309, 2008.

[12] R. Caldwell *et al.*, "Neural electrode resilience against dielectric damage may be improved by use of highly doped silicon as a conductive material," *J. Neurosci. Methods*, vol. 293, pp. 210–225, 2018.

[13] S. F. Cogan, J. Ehrlich, T. D. Plante, and R. Van Wagenen, "Penetrating microelectrode arrays with low-impedance sputtered iridium oxide electrode coatings," in *2009 Annual International Conference of the IEEE Engineering in Medicine and Biology Society*, Sep. 2009, pp. 7147–7150.

[14] S. Negi, R. Bhandari, and F. Solzbacher, "Morphology and Electrochemical Properties of Activated and Sputtered Iridium Oxide Films for Functional Electrostimulation," *J. Sens. Technol.*, vol. 02, no. 03, pp. 138–147, 2012.

[15] K. A. Ludwig, J. D. Uram, J. Yang, D. C. Martin, and D. R. Kipke, "Chronic neural recordings using silicon microelectrode arrays electrochemically deposited with a poly(3,4-ethylenedioxythiophene) (PEDOT) film," *J. Neural Eng.*, vol. 3, no. 1, pp. 59–70, 2006.

[16] P. Takmakov, K. Ruda, K. Scott Phillips, I. S. Isayeva, V. Krauthamer, and C. G. Welle, "Rapid evaluation of the durability of cortical neural implants using accelerated aging with reactive oxygen species," *J. Neural Eng.*, vol. 12, no. 2, 2015.

[17] R. Caldwell, M. G. Street, R. Sharma, P. Takmakov, B. Baker, and L. Rieth, "Characterization of Parylene-C degradation mechanisms: In vitro reactive accelerated aging model compared to multiyear in vivo implantation," *Biomaterials*, vol. 232, no. December 2019, p. 119731, 2020.

[18] E. A. Feilat, S. Grzybowski, and P. Knight, "Accelerated aging of high voltage encapsulated transformers for electronics applications," in *Proceedings of the 6th International Conference on Properties and Applications of Dielectric Materials (Cat. No.00CH36347)*, 2000, vol. 1, no. 1, pp. 209–212.

[19] J. B. Bernstein, "Failure Mechanisms," in *Reliability Prediction from Burn-In Data Fit to Reliability Models*, Elsevier, 2014, pp. 31–48.